BRCORP
TECHNOLOGY | INNOVATION | INDUSTRY

5th World Conference on
Applied Sciences, Engineering& Technology
02-04 June 2016, HCMUT, Vietnam

Kinematic Modelling and Geometric Optimization of a Cable-driven Hand Exoskeleton for Haptic Applications

TIN HUU LE QUANG NGUYEN, VIET-HONG TRAN
Department of Mechatronic Engineering, Faculty of Mechanical Engineering,
Ho Chi Minh city University of Technology, VNU-HCM, Ho Chi Minh city, Vietnam
Email: 21203870@hcmut.edu.vn, tvhong@hcmut.edu.vn

Abstract: This paper describes kinematic model of a cable-driven hand exoskeleton and optimization of its geometry to meet primary performance requirements in haptic applications. Firstly, forward and inverse kinematics of both 2-link and 3-link finger configurations were derived. Then, an optimization problem to find proper lengths of the linkage, which maximize the efficiency of the drive system and the contact force at user's finger under mechanical design constraints, was stated and the solving procedure was proposed. Lastly, the optimal results were subjected to a collision detection algorithm to finalize the exoskeleton's geometry. The results will be the foundation for future studies on the design of cable routing system, contact force sensor system and drive system of the hand exoskeleton model.

Keywords: *Exoskeleton, Haptic, Kinematic, Cable-driven, Optimization*

Introduction:

Haptic interfaces attempt to replicate or enhance the touch experience of manipulating or perceiving a real environment through mechatronic devices and computer control **[1]**. For tasks requiring more dexterity and human experience is concerned, such as tele-manipulation **[2]**, virtual reality **[3]**, human assistive devices **[4]** and medical applications **[5]**, it may be necessary to control applied forces on independent fingers rather than at the wrist, as joysticks and master arms do **[6]**. Hand exoskeleton can be used as one kind of haptic device, which is worn on the user's hand and provides force feedback to the fingers.

A hand exoskeleton for haptic application should have two key functions: (1) to measure the kinematic configuration (position, velocity, acceleration) and contact forces of the user's fingers and (2) to display contact forces to the user **[7]**. As a force feedback user interface, the hand exoskeleton should be user-friendly and effectively apply force to the fingers. A "user-friendly" glove is ergonomic and lightweight with a compact design that does not harm fingers. An "effective" glove provides controllable contact forces ranging from a gentle touch to full opposition to finger movement without kinematic constraints on the finger movement **[8]**. However, existing hand exoskeleton devices for haptic applications have not fully satisfied these criteria. They either are bulky and heavy or only accommodate limited range of motions and maximum contact forces **[9-12]**.

In order to deliver a compact and lightweight hand exoskeleton, which is mounted on user's hand, it is crucial to choose an appropriate drive mechanism. The current drive system for hand exoskeleton can be divided into three main categories: linkage-based, soft actuator and cable-driven. While linkage-based mechanism boasts the highest rigidity and has linear force transmission, it is bulky, produce high stresses on supporting connectors and has complicated structure **[9-11]**. Soft-actuator-based mechanism has high compliance, low inherent stiffness, safer interaction and higher power to weight ratio, however, it has longer setup time, produces shear forces on attachment points and has limited degrees of freedom **[12-14]**. Cable-driven mechanism provides rigid mechanical body support, lightweight and compact structure; has linear force transmission and its actuators can be placed far away. Its shortcomings are that its efficiency is relatively lower than others (because of the friction along the transmission) and the complexity of cables' placement (because cable can only transmit forces when it is stretched) **[8, 15-18]**. Therefore, the mechanism to be used in this research for a lightweight and compact hand exoskeleton is cable-driven.

A hand exoskeleton which does not hinder any natural movements of the user can be delivered when we apply the knowledge about the special characteristics of human hand's degrees of freedom. A human finger (except thumb), without abduction/adduction movements, can be considered as a 3-bar linkage (*Figure 1)* with 3 revolute joints. However, due to the anatomical model of human finger, especially the tendons placements, there is constraint between PIP and DIP joints in active movements. This is an almost linear relationship **[19-20]**. However, this constraint can be destroyed when the contact force axis goes through MCP or the contact area is not just the fingertip, but the fingerpad.

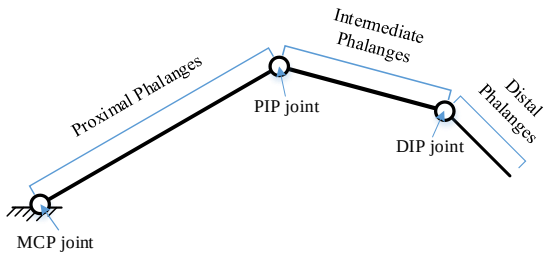

Figure 1: Model of a human finger.

In this paper we established two kinematic models of hand exoskeleton, 2-link and 3-link, which, respectively, can be used in cases where the contact the constraint between PIP and DIP is kept and not. Then, an example of the procedure to optimize the 3-link cable-driven exoskeleton's geometry in order to maximize drive system's efficiency and contact forces is done. Lastly, we discuss optimization result and describe future work.

Materials and Methods:

2-link model

This model makes use of the constraint between PIP and DIP. For each finger, the exoskeleton mechanism and the finger itself can be modelled as a single 5-bar mechanism, as shown in *Figure 2*, where the hand/support pad represents the ground. Each finger has 3 links, and the exoskeleton mechanism for each finger has 2 links. The terminal link of the exoskeleton is assumed to be rigidly connected to the terminal link of each finger. Therefore, the system consists of 5 links in total: 1 ground link, 3 finger links and 1 mechanism link; 4 revolute joints and one angular relation between PIP and DIP. According to Grubler's formula, the mobility of the system can be calculated, where *DF* is the system's degrees of freedom, $n = 5$ is the number of links, $f_1 = 5$ is the number of lower-pair (1DOF) joints and constraints, $f_2 = 0$ is the number of higher-pair joints:

$$DF = 3(n-1) - 2f_1 - f_2 = 2 \quad (1)$$

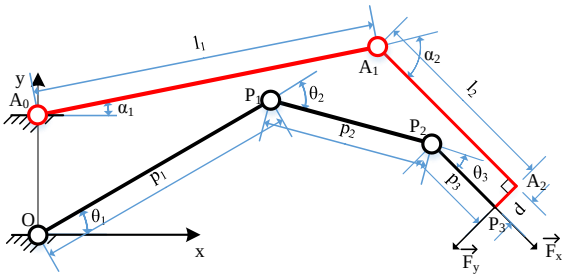

Figure 2: Kinematic diagram of 2-link model

Based on *Figure 2*, the forward kinematic equations for the fingertip position (x_{P_3}, y_{P_3}) are derived in Eqs. (2)–(4) in terms of the finger joint angles $(\theta_1, \theta_2, \theta_3)$ and the mechanism joint angles (α_1, α_2), where l_i is the length of the i^{th} mechanism link $\overline{A_{i-1}A_i}$, p_i is the length of the i^{th} finger link $\overline{P_{i-1}P_i}$, d is the length of $\overline{A_2P_3}$,. Note that *s* and *c* represent *sine* and *cosine*.

$$\begin{aligned} x_{P_3} &= p_1c_{\theta_1} + p_2c_{\theta_{12}} + p_3c_{\theta_{123}} \\ &= l_1c_{\alpha_1} + l_2c_{\alpha_{12}} + ds_{\alpha_{12}} \end{aligned} \quad (2)$$

$$\begin{aligned} y_{P_3} &= p_1s_{\theta_1} + p_2s_{\theta_{12}} + p_3s_{\theta_{123}} \\ &= y_{A_0} + l_1s_{\alpha_1} + l_2s_{\alpha_{12}} - dc_{\alpha_{12}} \end{aligned} \quad (3)$$

$$\phi = \theta_1 + \theta_2 = \alpha_1 + \alpha_2 + \alpha_3 \quad (4)$$

After solving (2)–(4), inverse kinematic equations, Eqs. (5)–(6), for mechanism joint angle (α_1, α_2) can be derived. Since the exoskeleton linkage is longer than the human finger, two solutions can be found: elbow up and elbow down configurations. The elbow up solution was chosen in order to avoid the collision between the finger and the linkage. In this case, the finger joint angles are prescribed.

$$\begin{aligned} \alpha_1 = atan2\left(\frac{y_{P_3} - y_{A_0}}{x_{P_3}}\right) \\ + acos\left(\frac{l_1^2 + x_{P_3}{}^2 + \left(y_{P_3} - y_{A_0}\right)^2 - \left(d^2 + l_2^2\right)}{2l_1\sqrt{x_{P_3}{}^2 + \left(y_{P_3} - y_{A_0}\right)^2}}\right) \end{aligned} \quad (5)$$

$$\begin{aligned} \alpha_2 = atan2\left(\frac{d}{l_2}\right) \\ - acos\left(\frac{x_{P_3}{}^2 + \left(y_{P_3} - y_{A_0}\right)^2 - l_1^2 - \left(d^2 + l_2^2\right)}{2l_1\sqrt{d^2 + l_2^2}}\right) \end{aligned} \quad (6)$$

The inverse kinematic equations, Eqs. (7)–(9), for the posture of user's finger $(\theta_1, \theta_2, \theta_3)$ can be derived, knowing the mechanism joint angles (α_1, α_2).

$$\theta_1 = \alpha_1 + \alpha_1 - \theta_3 - \theta_2 \quad (7)$$

$$\theta_2 = -acos\left(\frac{x_{P2}{}^2 + y_{P2}{}^2 - p_1^2 - p_2^2}{2p_1p_2}\right) \quad (8)$$

$$\theta_3 = \frac{2}{3}\theta_2 \quad (9)$$

Where Eq. (9) is derived from **[19]** and

$$x_{P_2} = x_{P_3} - p_3c_{\alpha_{12}} \quad (10)$$

$$x_{P_2} = x_{P_3} - p_3c_{\alpha_{12}} \quad (11)$$

3-link model

In this model, because of the loss constraint between PIP and DIP, *DF* of the system increases by 1, Eq. (12). Hence, a third exoskeleton's link is added in order to compensate. The system can be modelled as a single 6-bar mechanism, as shown in *Figure 3* with similar assumption and annotations as in the 2-link model. It consists of 6 links in total: 1 ground link, 3 finger links, 2 haptic mechanism links and 6 revolute joints. In this case, the mobility of the system can be recalculated with $n = 6$, $f_1 = 6$ and $f_2 = 0$:

$$DF = 3(n-1) - 2f_1 - f_2 = 3 \quad (12)$$

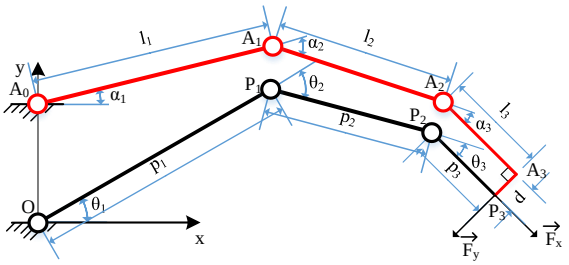

Figure 3: Kinematic diagram of 3-link model

Similarly, we can write the forward kinematic equations, Eqs. (13)–(15), and inverse kinematic equations, Eqs. (16)–(18), (21)–(23) ,for this model. Forward kinematic equations:

$$x_{P_3} = p_1 c_{\theta_1} + p_2 c_{\theta_{12}} + p_3 c_{\theta_{123}} = l_1 c_{\alpha_1} + l_2 c_{\alpha_{12}} + l_3 c_{\alpha_{123}} + d s_{\alpha_{123}} \quad (13)$$

$$y_{P_3} = p_1 s_{\theta_1} + p_2 s_{\theta_{12}} + p_3 s_{\theta_{123}} = y_{A_0} + l_1 s_{\alpha_1} + l_2 s_{\alpha_{12}} + l_3 c_{\alpha_{123}} - d c_{\alpha_{123}} \quad (14)$$

$$\phi = \theta_1 + \theta_2 + \theta_3 = \alpha_1 + \alpha_2 + \alpha_3 \quad (15)$$

Inverse kinematic equations for mechanism joint angles:

$$\alpha_1 = atan2\left(\frac{y_{A_2}}{x_{A_2}}\right) + acos\left(\frac{l_1^2 - l_2^2 + {x_{A_2}}^2 + {y_{A_2}}^2}{2l_1\sqrt{{x_{A_2}}^2 + {y_{A_2}}^2}}\right) \quad (16)$$

$$\alpha_2 = -acos\left(\frac{{x_{A2}}^2 + {y_{A2}}^2 - l_1^2 - l_2^2}{2l_1 l_2}\right) \quad (17)$$

$$\alpha_3 = \theta_1 + \theta_2 + \theta_3 - \alpha_1 - \alpha_2 \quad (18)$$

Where

$$x_{A_2} = x_{P_3} - d s_{\theta_{123}} - l_3 c_{\theta_{123}} \quad (19)$$

$$y_{A_2} = y_{P_3} + d c_{\theta_{123}} - l_3 s_{\theta_{123}} - y_{A_0} \quad (20)$$

Inverse kinematic equations for finger joint angles:

$$\theta_1 = atan2\left(\frac{y_{P_2}}{x_{P_2}}\right) + acos\left(\frac{p_1^2 - p_2^2 + {x_{P_2}}^2 + {y_{P_2}}^2}{2p_1\sqrt{{x_{P_2}}^2 + {y_{P_2}}^2}}\right) \quad (21)$$

$$\theta_2 = -acos\left(\frac{{x_{P_2}}^2 + {y_{P_2}}^2 - p_1^2 - p_2^2}{2p_1 p_2}\right) \quad (22)$$

$$\theta_3 = \alpha_1 + \alpha_2 + \alpha_3 - \theta_1 - \theta_2 \quad (23)$$

Where

$$x_{P_2} = x_{P_3} - p_3 c_{\alpha_{123}} \quad (24)$$

$$y_{P_2} = y_{P_3} - p_3 s_{\theta_{123}} \quad (25)$$

Example of 3-link cable-driven exoskeleton's geometry optimization

The linkage geometry optimization problem for a 3-link cable-driven hand exoskeleton was proposed in **[8]**. It is a multi-objective optimization function, Eq. (26), with force transmission ratio objective function z_1, Eq. (27), and contact force objective function z_2, Eq. (28).

$$Z = w_1 z_1 + w_2 z_2 \quad (26)$$

Where $w_1 = w_2 = 1$ are the weighting coefficients.

$$z_1 = \sqrt{\alpha_{1,var}^2 + \alpha_{2,var}^2 + \alpha_{3,var}^2} \quad (27)$$

Where $a_{i,var} = a_{i,max} - a_{i,min}, i \in \{1,2,3\}$ is the range of mechanism joint angle α_i with a given set of exoskeleton links' length (l_1, l_2, l_3).

$$z_2 = \sqrt{\alpha_{21}^2 + \alpha_{22}^2 + \alpha_{23}^2} \quad (28)$$

Where

$$\alpha_{21} = l_1 c_{\alpha_1} + l_2 c_{\alpha_{12}} + l_3 c_{\alpha_{123}} + d s_{\alpha_{123}} \quad (29)$$

$$\alpha_{22} = l_2 c_{\alpha_{12}} + l_3 c_{\alpha_{123}} + d s_{\alpha_{123}} \quad (30)$$

$$\alpha_{23} = l_3 c_{\alpha_{123}} + d s_{\alpha_{123}} \quad (31)$$

The constraints for this optimization problem **[8]** were stated based on limitations in kinematic configurations, Eq. (32), mechanical design, Eq. (33), and the collision-free operational requirement, Eq. (34).

$$c_1 : l_1 + l_2 + l_3 > p_1 + p_2 + p_3 \quad (32)$$

$$c_2 : a_{i,var} \le 150^o, i \in \{1,2,3\} \quad (33)$$

$$c_1 : l_1 > p_1 \quad (34)$$

In this paper, we propose a Monte Carlo approach to solve this optimization problem:

- *Step 1:* Establish searching range for (l_1, l_2, l_3) and user's range of motions for each joint angle. The constraint between PIP and DIP $\left(\theta_3 = \frac{2}{3}\theta_2\right)$ is kept due to it is satisfied in most of normal operations.
- *Step 2:* Choose one set of (l_1, l_2, l_3).
- *Step 3:* Calculate values of $(\alpha_1, \alpha_2, \alpha_3)$ and z_2 for each set of $(\theta_1, \theta_2, \theta_3)$.
- *Step 4:* Calculate z_1
- *Step 5:* Calculate Z. If all set of (l_1, l_2, l_3) has been chosen, go to *Step 6*, else, go to *Step 2*.
- *Step 6:* Remove all complex Z values, which are caused by having any complex α_i during the calculation.
- *Step 7:* Applying constraints to the rest of Z values to remove any unsatisfied value.
- *Step 8:* Choose the minimum Z value and corresponding set of (l_1, l_2, l_3).
- *Step 9:* Detecting collisions between mechanism links and user's finger with the chosen set of (l_1, l_2, l_3) by looking for any intersection with every set of $(\theta_1, \theta_2, \theta_3)$. This time, the constraint between θ_2 and θ_3 is abolished. If collision is detected, remove the set of (l_1, l_2, l_3) and the corresponding Z and go to *Step 8*, else, choose that set as the final values.

Results and Discussion:

The optimization procedure was done with author's index finger dimension and the range of motion, *Table 1*, $d = 5mm$, $y_{A_0} = 20mm$. The searching range was from (p_1, p_2, p_3) to $(2p_1, 2p_2, 2p_3)$ **[8]**. The final result is shown in *Table 2*

Table 1: Author's index finger dimension and workspace

Finger joint	Angular motion range (deg)	Finger link length (mm)
MCP	[-90;30]	45
PIP	[-120;0]	28
DIP	[-80;0]	13

Table 2: Optimization result

Exoskeleton joint	Angular motion range (deg)	Finger link length (mm)
A_1	[-77.5; 67.3]	45.1
A_2	[-117.6;0]	48.1
A_3	[-20.8; 88.6]	14

We examined the result by drawing the workspace of user's finger and exoskeleton using the joint angle sweep method, *Figure 4*. The figure shown that the workspace of user's finger was a subset of the mechanism's workspace, ensuring unhindered finger motion. This result is different from which acquired in **[8]** because of the differences in target finger dimensions, searching range and the application of PIP-DIP constraint during the optimization.

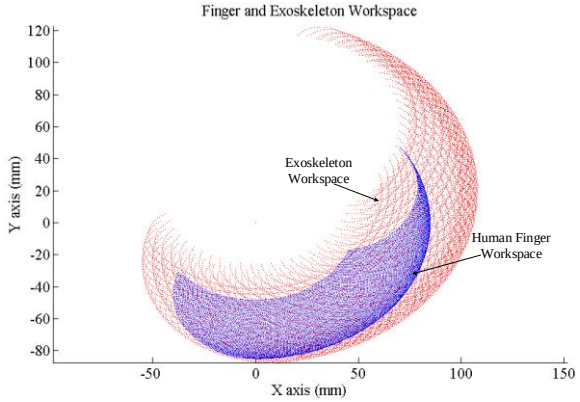

Figure 4: 2D workspace comparison between index finger and the exoskeleton mechanism when l = [45.1;48.1;14], α_1 = [-80;70], α_2 = [-120;0], α_1 = [-25;90].

Conclusion:

This paper has shown the kinematic models of 2-link and 3-link cable-driven hand exoskeleton and their working condition; proposed a Monte Carlo approach for the mechanism geometry optimization problem and applied it to solve for the links length of an index finger mechanism. The optimal result was examined to verify the algorithm.

Future work will be devoted to the design of cable routing system, contact force sensor system and drive system of a 3-link cable-driven hand exoskeleton for haptic application.

References:

[1] Khatib, O., and Siciliano, B., (2008) "Springer Handbook of Robotics", Springer, Berlin, Germany.

[2] Fang, H., Xie, Z., and Liu, H., (2009) "An Exoskeleton Master Hand for Controlling DLR/HIT Hand," IEEE/RSJ International Conference on Intelligent Robots and Systems (IROS 2009), St. Louis, MO, Oct. 10–15, pp. 3703–3708.

[3] Jack, D., Boian, R., Merians, A. S., Tremaine, M., Burdea, G. C., Adamovich, S. V., Reece, M., and Poizner, H., (2001) "Virtual Reality Enhanced Stroke Rehabilitation," IEEE Trans. Neural Syst. Rehabil. Eng., 9(3), pp. 308–318.

[4] Luo, X., Kline, T., Fischer, H., Stubblefield, K., Kenyon, R., and Kamper, D., (2005) "Integration of Augmented Reality and Assistive Devices for Post-Stroke Hand Opening Rehabilitation," IEEE-EMBS 27th Annual International Conference of the Engineering in Medicine and Biology Society (IEEE-EMBS 2005), Shanghai, China, Sept. 1–4, pp. 6855–6858.

[5] Popescu, V. G., Burdea, G. C., Bouzit, M., and Hentz, V. R., (2000) "A VirtualReality-Based Telerehabilitation System with Force Feedback," IEEE Trans. Inf. Technol. Biomed., 4(1), pp. 45–51.

[6] Burdea, G., and Coiffet, P., (2003) "Virtual Reality Technology", Vol. 1, 2nd ed., Wiley, New York, p. 107.

[7] Tan, H. Z., Srinivasan, M. A., Eberman, B., and Cheng, B., (1994) "Human Factors for the Design of Force-Reflecting Haptic Interfaces," ASME Dyn. Syst. Control, 55(1), pp. 353–359.

[8] Ma Z and Ben-Tzvi P., (2015) "Design and Optimization of a Five-Finger Haptic Glove Mechanism", ASME. J. Mechanisms Robotics, 7(4), p. 041008.

[9] Susanto, E. A., Tong, R. K., and Ho, N. S., (2015) "Hand exoskeleton robot for assessing hand and finger motor impairment after stroke", HKIE Transactions, 22(2), pp. 78-87.

[10] Bi, Q., Yang, C. J., Deng, X. L., and Fan, J. C., (2015) "Human finger mechanical impedance modeling: Using multiplicative uncertain model", Proceedings of the Institution of Mechanical Engineers, Part C: Journal of Mechanical Engineering Science, p. 0954406215587343

[11] Iqbal, J., Tsagarakis, N.G. and Caldwell, D.G., (2015) "Four-fingered lightweight exoskeleton robotic device accommodating different hand sizes", Electronics Letters, 51(12), pp.888-890.

[12] Yap, H. K., Lim, J. H., Nasrallah, F., Goh, J. C., and Yeow, R. C., (2015) "A soft exoskeleton for hand assistive and rehabilitation application using pneumatic actuators with variable stiffness", Robotics and Automation (ICRA),

2015 IEEE International Conference, pp. 4967-4972. IEEE.

[13] Hasegawa, Y. and Suzuki, T., (2015) "Thin and active fixture to hold finger for easy attachment and comfort of grasping support exoskeleton", Robotics and Automation (ICRA), 2015 IEEE International Conference, pp. 4973-4978. IEEE.

[14] Thompson-Bean, E., Steiner, O. and McDaid, A., (2015) "A soft robotic exoskeleton utilizing granular jamming", Advanced Intelligent Mechatronics (AIM), 2015 IEEE International Conference, pp. 165-170. IEEE.

[15] Lee, S., Landers, K.A. and Park, H.S., (2014) "Development of a biomimetic hand exotendon device (BiomHED) for restoration of functional hand movement post-stroke", Neural Systems and Rehabilitation Engineering, IEEE Transactions, *22*(4), pp.886-898.

[16] In, H., Kang, B.B., Sin, M. and Cho, K.J., (2015) "Exo-Glove: a wearable robot for the hand with a soft tendon routing system", Robotics & Automation Magazine, IEEE, 22(1), pp.97-105.

[17] Yang, J., Xie, H. and Shi, J., (2016) "A novel motion-coupling design for a jointless tendon driven finger exoskeleton for rehabilitation", Mechanism and Machine Theory, 99, pp.83-102.

[18] Lau, D., Oetomo, D. and Halgamuge, S.K., (2013) "Generalized modeling of multilink cable-driven manipulators with arbitrary routing using the cable-routing matrix", Robotics, IEEE Transactions on, 29(5), pp.1102-1113.

[19] Lee, J. and Kunii, T.L., (1995) "Model-based analysis of hand posture", Computer Graphics and Applications, IEEE, 15(5), pp.77-86.

[20] Becker, J.C. and Thakor, N.V., (1988) "A study of the range of motion of human fingers with application to anthropomorphic designs", Biomedical Engineering, IEEE Transactions, 35(2), pp.110-117.